Available online at www.sciencedirect.com

SCIENCE DIRECT®

ELSEVIER

Journal of the European Ceramic Society 26 (2006) 1913–1916

ECERS

www.elsevier.com/locate/jeurceramsoc

Microstructure and dielectric properties of the Ti-rich $BaO–TiO_2$ thin films for microwave devices

Bo-Yun Jang[a], Young-Hun Jeong[a], Suk-Jin Lee[a], Kyong-Jae Lee[a], Sahn Nahm[a,*], Ho-Jung Sun[b], Hwack-Joo Lee[c]

[a] *Department of Materials Science and Engineering, Korea University, 1-5 Ka, Anam-Dong, Sungbuk-Ku, Seoul 136-701, South Korea*
[b] *Department of Materials Science and Engineering, Kunsan National University, Kunsan, 573-701, South Korea*
[c] *New Materials Evaluation Center, Korea Research Institute of Standards and Science, Daeduk Science Town, Taejon 305-600, South Korea*

Abstract

Ti-rich $BaO–TiO_2$ thin films were grown on a $Pt/Ti/SiO_2/Si$ substrate using rf sputtering and the structural and dielectric properties of the films were investigated. For the film grown at room temperature and rapidly thermal annealed (RTA) at 900 °C for 3 min, an amorphous phase with a small $BaTi_5O_{13}$ crystalline phase was formed. As the growth temperature increased, the amount of the $BaTi_5O_{11}$ crystalline phase increased. For the film grown at 350 °C and RTA at 900 °C for 3 min, the homogeneous $BaTi_5O_{11}$ phase was formed. The $BaTi_4O_9$ phase was developed when the growth temperature exceeded 450 °C. The thin film with the homogeneous $BaTi_4O_9$ phase was obtained when the film was grown at 550 °C and RTA at 900 °C for 3 min. The dielectric properties of the films were measured at 1–6 GHz range. The dielectric constant (ϵ_r) of the $BaTi_5O_{11}$ film was about 33 and the dissipation factor was about 0.01. The ϵ_r and the dissipation factor of the $BaTi_4O_9$ film were about 37 and 0.005, respectively.

Keywords: Films; Microstructure; Dielectric properties; Capacitors; Ti-rich $BaO–TiO_2$

---

1. Introduction

Next generation technologies of wireless and satellite communications require small-sized microwave devices operating at low power. Miniaturization of the devices can be achieved by the development of microwave integrated circuits (MICs) of active and passive devices. It is generally known that various MICs of active devices have been developed using transistors. However, the MIC of the passive devices has rarely been developed and this can be achieved by using thin film microwave materials, which have a high ϵ_r, a low loss and good temperature stability. Therefore, investigations on the microwave thin films have been increased.[1,2]

The Ti-rich $BaO–TiO_2$ system has been extensively studied because this system has many compounds, which have excellent microwave dielectric properties.[3–5] The $BaTi_4O_9$ phase was first reported by Satton et al.[3] and the crystal structure of this phase was identified as a orthorhombic with lattice parameters of $a = 1.453$ nm, $b = 0.379$ nm and $c = 0.629$ nm.[6] The $BaTi_4O_9$ ceramic shows the good microwave dielectric properties of $Q = 2500–5000$, $\epsilon_r = 36–39$ at 4–10 GHz and the temperature coefficient of the resonance frequency $(\tau_f) < 20$ ppm/°C.[4,5] The $Ba_2Ti_9O_{20}$ ceramic is also known to have excellent microwave dielectric properties, especially the τ_f value is nearly zero.[7] However, it is difficult to obtain a single $Ba_2Ti_9O_{20}$ phase.[8] The $BaTi_5O_{11}$ phase was first formed from a quenched melt of $BaTi_4O_9$.[9] The single $BaTi_5O_{11}$ phase was not produced from the solid-state reaction but it was only synthesized by the solution method.[10] All the previous works on the Ti-rich $BaO–TiO_2$ system have concentrated on the bulk ceramics but no research has been carried out on the structural and dielectric properties of the thin film. In this work, the $BaTi_4O_9$ and $BaTi_5O_{11}$ films were grown on a $Pt/Ti/SiO_2/Si$ substrate using rf magnetron sputtering and the structural and dielectric properties of the thin films at GHz range were investigated.

2. Experimental procedure

Thin films were grown on a $Pt/Ti/SiO_2/Si$ substrate by rf magnetron sputtering using a $BaTi_4O_9$ target with a 3 in. diameter which was synthesized by the conventional solid state method. The background pressure was approximately 10^{-7} Torr and the sputtering was conducted in an oxygen and argon (O_2:Ar = 1:4)

---

[*] Corresponding author. Fax: +82 2 928 3584.
E-mail address: snahm@korea.ac.kr (S. Nahm).

0955-2219/$ – see front matter © 2005 Elsevier Ltd. All rights reserved.
doi:10.1016/j.jeurceramsoc.2005.09.020

atmosphere with a total pressure of 8 mTorr. The rf power was 100 W and the substrate temperature was controlled from room temperature to 550 °C using a pedestal-type heater. After the deposition, the films were subjected to a rapidly thermal annealing at 900 °C under O_2 atmosphere. The working pressure of the annealing was 3–5 Torr. The microstructure was analyzed using X-ray diffraction (Rigaku D/max-RC, Japan) and transmission electron microscopy (TEM: Hitachi H-9000NAR Ibaraki, Japan). For the measurement of the dielectric properties at microwave frequencies, Al was deposited on the thin film as the top electrode using conventional dc sputtering. The Al-electrode was patterned to form a circular-patch capacitor structure by photolithography. The complex reflection coefficient was measured from 1 to 6 GHz using a Vector Network Analyzer (HP 8710C). The dielectric constant and the dissipation factor were calculated from two reflection coefficients of capacitors having different inner diameters with the same outer diameters.[11]

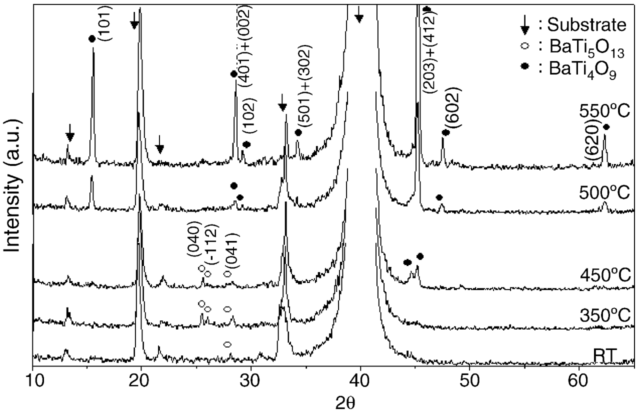

Fig. 1. X-ray diffraction patterns of the thin films grown at various temperatures for 1 h and rapidly thermal annealed at 900 °C for 3 min.

3. Results and discussion

Fig. 1 shows the X-ray diffraction patterns of the thin films grown at various temperatures and subsequently rapidly thermal annealed (RTA) at 900 °C for 3 min. For the film grown at room temperature a small peak indexed as a (0 4 1) reflection of monoclinic $BaTi_5O_{11}$ phase appeared. As the growth temperature increased, the amount of the $BaTi_5O_{11}$ phase also increased. However, when the growth temperature was 450 °C, the peaks corresponding to the $BaTi_4O_9$ phase appeared, thus thin film grown at 450 °C and RTA at 900 °C consisted of the $BaTi_5O_{11}$ and the $BaTi_4O_9$ phases. When the growth temperature exceeded 450 °C, peaks for the $BaTi_5O_{11}$ phase disappeared and only those for the $BaTi_4O_9$ phase were observed. All the peaks were matched with those of the orthorhombic $BaTi_4O_9$ phase. From these results, it can be suggested that a crystalline $BaTi_5O_{11}$ phase is formed when the growth temperature is lower than 450 °C and a $BaTi_4O_9$ phase is crystallized when the growth temperature is above 450 °C.

In order to understand the crystallization behavior of the Ti-rich BaO–TiO_2 thin films, HRTEM analysis was conducted. Fig. 2(a) shows a HRTEM image of the thin film grown at room temperature and RTA at 900 °C for 3 min. The inset shows the electron diffraction pattern taken from the same area of the film. The ring pattern indexed as the (0 4 1) reflection of the $BaTi_5O_{11}$ phase indicates that the grain size of the $BaTi_5O_{11}$ phase is very small. The modulation of the (0 4 1) lattice plane corresponding to 0.32 nm was shown in HRTEM image and an amorphous phase indicated by A was also observed in this image. Therefore,

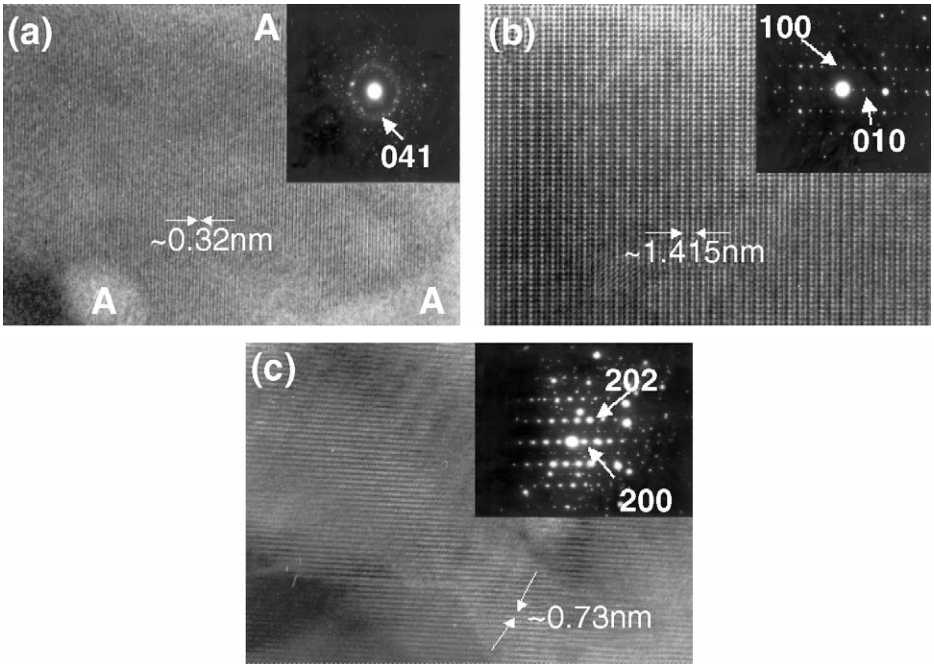

Fig. 2. High-resolution lattice images and the electron diffraction patterns of the thin films grown at: (a) room temperature, (b) 350 °C and (c) 550 °C for 1 h and rapidly thermal annealed at 900 °C for 3 min.

the film grown at room temperature and RTA at 900 °C consists of the small $BaTi_5O_{11}$ grains and the amorphous phase. The HRTEM image and electron diffraction pattern of thin film grown at 350 °C and RTA at 900 °C were illustrated in Fig. 2(b). The electron diffraction pattern was identified as the [0 0 1] zone axis diffraction patterns of the $BaTi_5O_{11}$ phase. The modulation of (0 1 0) lattice plane with wavelength of 1.415 nm was shown in the HRTEM image, and it is difficult to find the amorphous phase. Therefore, thin film grown at 350 °C and RTA at 900 °C is fully crystallized $BaTi_5O_{11}$ phase. Fig. 2(c) is the HRTEM image and electron diffraction patterns of thin film grown at 550 °C and RTA at 900 °C. The inset shows the [0 4 0] zone axis electron diffraction pattern of the $BaTi_4O_9$ phase. The HRTEM image also shows the modulation of the (2 0 0) lattice plane of $BaTi_4O_9$ phase. TEM analysis shows that although the composition of the sputtering target is $BaTi_4O_9$, the $BaTi_5O_{11}$ phase is formed when the growth temperature is low, and a high growth temperature is required to obtain the crystalline $BaTi_4O_9$ phase.

In the case of bulk ceramics, the $BaTi_5O_{11}$ phase was first found in the quenched melt of $BaTi_4O_9$ by Tillmanns.[9] The $BaTi_5O_{11}$ phase was also produced by sol–gel or liquid mixture method but it was never produced from the solid state method.[10] Therefore, it is thought that the $BaTi_5O_{11}$ phase was obtained only from the amorphous phase. Moreover, when the ratio of BaO and TiO_2 was 1:4 in the precursor solution in the sol–gel method, the $BaTi_5O_{11}$ phase existed as the low temperature phase and transformed into the $BaTi_4O_9$ phase when the annealing temperature was 1300 °C.[10] In the case of thin film, only amorphous phase formed when the film was grown at room temperature. The composition of this amorphous film might be close to $BaTi_4O_9$ because the sputtering target is $BaTi_4O_9$. Therefore, the film grown at room temperature could be crystallized into the low temperature phase, i.e. $BaTi_5O_{11}$ phase when the annealing temperature was not high enough as shown in Fig. 2(a).

For the film grown at 350 °C, it is considered that the amorphous phase was developed during the deposition, and they changed to the $BaTi_5O_{11}$ phase. But it is also possible that the $BaTi_5O_{11}$ phase was already formed during the deposition, and they grew when the annealing was conducted. In order to identify the phase of film grown at 350 °C, TEM analysis was conducted. The dark field image of thin film grown at 350 °C was shown in Fig. 3. The inset shows the electron diffraction pattern taken at the same area. The ring patterns shown in the electron diffraction pattern are identified as the (0 3 2), (3 2 0) and (1 0 5) reflections of the $BaTi_5O_{11}$ phase. The dark field image shows that a small crystalline $BaTi_5O_{11}$ phase with average grain size of 10 nm formed and the amorphous phase was also detected in the dark field image. Therefore, it is considered that for the film grown at 350 °C, both a small crystalline $BaTi_5O_{11}$ phase and an amorphous phase are formed during the deposition and $BaTi_5O_{11}$ phase grows when the annealing is conducted.

In order to identify the phase of the film grown above 450 °C, TEM analysis was conducted on the film grown at 550 °C. Fig. 4 shows the dark field image of the film grown at 550 °C and the inset shows the electron diffraction pattern taken from the same area. The electron diffraction pattern shows the ring pattern indicating that the grain size is small. The first and second rings were indexed as the (3 1 0), and the (2 1 4) reflections of the $BaTi_4O_9$ phase, respectively. The dark field image exhibits the grains with an average grain size of 30–50 nm. Therefore, for the film grown at 550 °C, the small grains of the $BaTi_4O_9$ phase formed during the deposition, which grew during the post-annealing.

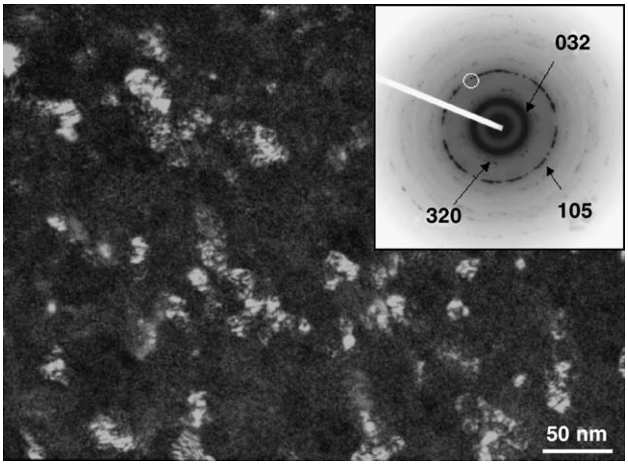

Fig. 3. Dark field image and electron diffraction pattern of the thin film grown at 350 °C for 1 h.

Dielectric properties of the thin films grown at the various temperatures and RTA at 900 °C were measured at 1–6 GHz as shown in Fig. 5. For the film grown at room temperature, the ϵ_r was low, about 25. Since the film grown at room temperature contains a large amount of the amorphous, the low ϵ_r value can be explained by the presence of the amorphous phase. The dissipation factor of the film was low, about 0.01 when it was measured below 3 GHz. However, it considerably increased at 3–6 GHz range. The increase of the dispassion factor is not clearly understood at this moment. The dielectric constants of the $BaTi_5O_{11}$ and $BaTi_4O_9$ thin films were 33 and 37 at 1–6 GHz, respectively. They are similar to those of the bulk specimens. The dissipation factor of the $BaTi_5O_{11}$ was about 0.01 at 1–4.5 GHz and it increased when the frequency exceeded 4.5 GHz. On the other hand, for the $BaTi_4O_9$ thin film, the dissipation factor was about 0.005 at 1–6 GHz. Therefore, $BaTi_4O_9$ thin film grown

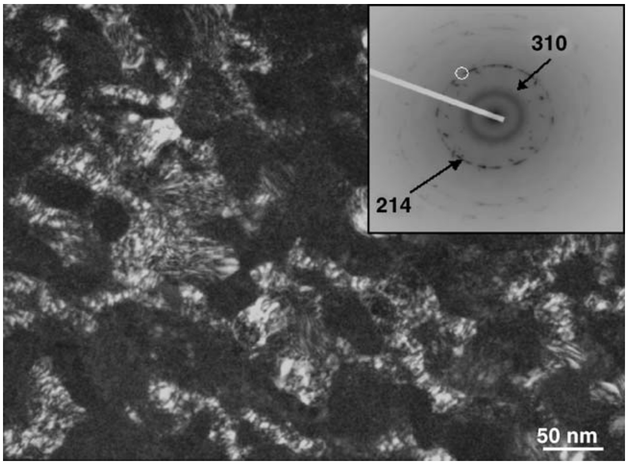

Fig. 4. Dark field image and electron diffraction pattern of the thin film grown at 550 °C for 1 h.

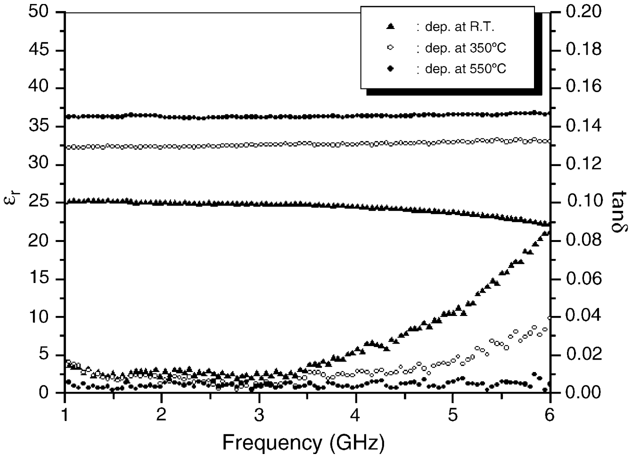

Fig. 5. Dielectric constants and dissipation factors of the thin films grown at the various temperatures and rapidly thermal annealed at 900 °C for 3 min.

at 550 °C and RTA at 900 °C is considered to have the good dielectric properties at 1–6 GHz range.

4. Conclusions

For the thin film grown at room temperature and RTA at 900 °C, amorphous phase was formed during the deposition and changed to the $BaTi_5O_{11}$ phase during the annealing. Thin film grown at 350 °C consisted of small $BaTi_5O_{11}$ grains, which grew when the film was RTA at 900 °C. For the film grown at 550 °C and RTA at 900 °C, the small $BaTi_4O_9$ crystalline phases were already formed during the deposition and they grew when annealing was conducted at 900 °C. The ϵ_r of the $BaTi_5O_{11}$ thin film was about 33, which is close to that of the bulk ceramics, and the dissipation factor was 0.01 and increased when the frequency exceeded 4.5 GHz. The ϵ_r and the dissipation factor of the $BaTi_4O_9$ thin film were 37 and 0.005 at 1–6 GHz, respectively. Therefore, the $BaTi_4O_9$ thin film could be applicable to microwave thin film devices.

Acknowledgments

This work was supported by the Ministry of Science and Technology through the project of Nano-Technology and one of the authors also acknowledges that this work was financially supported by the Ministry of Science and Technology through the NRL project.

References

1. Lee, B. D., Yoon, K. I., Kim, E. S. and Kim, T. H., Microwave dielectric properties of $CaTiO_3$ and $MgTiO_3$ thin films. *Jpn. J. Appl. Phys.*, 2003, **42**, 6158–6161.
2. Kim, Y., Oh, J., Kim, T. G. and Park, B., Effect of microstructures on the microwave dielectric properties of $ZrTiO_4$ thin films. *Appl. Phys. Lett.*, 2001, **78**(16), 2363–2365.
3. Statton, W. O., The phase diagram of the BaO–TiO_2 system. *J. Chem. Phys.*, 1951, **19**(1), 33–40.
4. Negas, T., Yeager, G., Bell, S., Coats, N. and Minis, I., $BaTi_4O_9$/$Ba_2Ti_9O_{20}$-based ceramics resurrected for modern microwave applications. *J. Am. Ceram. Soc. Bull.*, 1993, **72**, 80–89.
5. Choy, J.-H., Han, Y.-S., Sohn, J.-H. and Itoh, M., Microwave characteristics of BaO–TiO_2 ceramics prepared via a citrate route. *J. Am. Ceram. Soc.*, 1995, **78**, 1169–1172.
6. Templeton, D. H. and Dauben, C. H., Polarized octahedra in barium tetratitanate. *J. Chem. Phys.*, 1960, **32**(5), 1515–1518.
7. O'Bryan Jr., H. M., Thomson Jr., J. and Plourde, J. K., A new BaO–TiO_2 compound with temperature-stable high permittivity and low microwave loss. *J. Am Ceram. Soc.*, 1974, **57**(10), 450–453.
8. Xu, Y., Chen, X. M. and Wang, L., Sol–gel preparation of $BaTi_4O_9$ and $Ba_2Ti_9O_{20}$. *J. Am. Ceram. Soc.*, 2001, **84**, 669–671.
9. Tillmanns, V. E., Die Kristallstruktur Von $BaTi_5O_{11}$. *Acta Crystallogr. Sect. B*, 1969, **259**(Pt. 8), 1444–1452.
10. Ritter, J. J., Roth, R. S. and Blendell, J. E., Alkoxide precursor synthesis and characterization of phase in the barium–titanium oxide system. *J. Am. Ceram. Soc.*, 1986, **69**(2), 155–162.
11. Ma, Z., Becker, A. J., Polakos, P., Huggins, H., Pastalan, J., Wu, H. *et al.*, RF measurement technique for characterizing thin dielectric films. *IEEE Trans. Electron Devices*, 1998, **45**, 1811–1815.